Electron Transfer within an Antioxidant Powder Composite with Layered Double Hydroxide Nanoparticles and Tomato Extract

Rosa Nallely Murillo Vazquez [1], Citlali Pereyra Nuñez [1], Vadym Kovalenko [2], Valerii Kotok [3], Fermín Paul Pacheco Moisés [1], Adriana Macaria Macias Lamas [4], Gregorio Guadalupe Carbajal Arízaga [1,*]

[1] Chemistry Department, University of Guadalajara. Marcelino Garcia Barragán 1421. Postal code 44430, Guadalajara, Jalisco, Mexico; nallely.mv@gmail.com (R.N.M.V.); citlalip58@gmail.com (C.P.N.); ferminpacheco@hotmail.com (F.P.P.M.); gregoriocarbajal@yahoo.com.mx (G.G.C.A.);

[2] Department of Analytical Chemistry and Chemical Technology of Food Additives and Cosmetics, Ukrainian State University of Chemical Technology, 8, Gagarin Ave. Postal code 49005, Dnipro, Ukraine.; vadimchem@gmail.com (V.K.);

[3] Department of Processes, Apparatus and General Chemical Technology, Ukrainian State University of Chemical Technology, 8, Gagarin Ave. Postal code 49005, Dnipro, Ukraine.; valeriykotok@gmail.com (V.K.);

[4] Pharmacobiology Department, University of Guadalajara. Marcelino Garcia Barragán 1421. Postal code 44430, Guadalajara, Jalisco, Mexico; amaciaslamas@yahoo.com (A.M.M.L.);

* Correspondence: gregoriocarbajal@yahoo.com.mx (G.G.C.A.);

Abstract: Antioxidants are demanded compounds in the polymer, cosmetics, food, and health industry. Preparation of composites with antioxidants and layered double hydroxides (LDH) is a strategy to optimize antioxidant function and facilitate its addition to commercial products; therefore, understanding the antioxidant behavior of new antioxidant composites is needed to define and design the applications. We report a composite formed by $MgAl-NO_3$ layered double hydroxide nanoparticles spread along a lycopene matrix extracted from a tomato. Electron paramagnetic resonance (EPR) spectroscopy followed the reaction of hydroxyl radicals with the antioxidant composite material. The composite was reacted with different volumes of 30% H_2O_2 solution. Initially, the organic fraction of the composite reacts with OH· radicals and forms organic free radicals (OFR) detected with g = 2.009 in the EPR spectra. As the amount of OH· reacting with the composite increased, the intensity of OFR also increased; later, the unpaired electrons migrated to the $MgAl-NO3$ LDH nanoparticles, producing a new absorption signal with g = 2.020 in the EPR spectrum. This signal was assigned to the reduction of aluminum sites in the LDH. LDH particles are suitable components to increase the antioxidant performance composites produced with natural compounds.

Keywords: tomato; lycopene; composite; free radical; antioxidants.

1. Introduction

Antioxidants are demanded substances to retard or prevent damages caused by oxidation either in biological systems or materials. Respiration produces a chain of reactive oxygen species (ROS) in biosystems. Healthy organisms maintain an equilibrium between ROS formation and the activity of antioxidants so that the toxicity of ROS is reduced to the minimum level [1]. However, some diseases have been associated with an abnormal ROS concentration, which can be mitigated with antioxidants. For instance, natural antioxidants like

lycopene alleviate neurodegenerative and cardiovascular diseases [2–4] and reduce the risk of prostate, lung, and stomach cancer [5–8].

Regarding material science, polymeric materials can be degraded by the action of UV light, where free radicals are formed [9]; thus, antioxidants are added to neutralize them. Furthermore, adding antioxidants, such as lycopene, especially in biodegradable polymeric packing films [10], is a promising strategy to protect foods against oxidation. The addition of antioxidants has been tested successfully in biopolymers such as starch, whey protein, chitosan, polyvinyl alcohol, and poly-lactic acid, where mechanical and antioxidant properties were improved [11–16]. Additionally, the antioxidant activity of natural colored pigments can also be exploited to design biopolymers for food packaging with the capability of food spoilage detection [16].

Lycopene has been described as an effective natural antioxidant due to the many double bonds that react and neutralize ROS and free radicals [17,18]. As lycopene is one of the most effective natural antioxidants [17], we explored an alternative method to remove it from tomato juice through an environmentally friendly process with layered double hydroxides (LDH). An intermediate product in this process is a composite material formed by an intimate mixture of organic matter from tomato and LDH particles; the solid tomato extract (TE) in this composite contains lycopene [19]. In this article, we explore the antioxidant behavior of this intermediate, considering that LDH composite can be used as an antioxidant composite either as filler in polymers or even nutraceutical.

LDH are inorganic powders formed by layered units of hydroxide metals with a residue of positive charge, which is stabilized with interlayer anions [20]. The composition of LDH is represented by the formula: $[M(II)_{1-x}M(III)x(OH)_2]^{x+} (A^{n-})_{x/n} \cdot mH_2O$, where M(II) and M(III) are di- and trivalent metal cations respectively, and A^{n-} is the interlayer anion [21,22]. As A^{n-} is exchangeable, scientists have prepared an extensive range of composites by combining properties from the LDH and the new anion. For example, the co-existence of anions derived from acid green 25 and acid yellow 25 dyes in the interlayer space of an LDH allows for tuning the color of the composite pigment due to electron exchange between dyes molecules and also between dyes and the LDH; additionally, the composite increased the thermal resistance and regulated hydrophobicity [12]. Therefore, considering that LDH modifies the organic component properties when forming composites, this work aimed to study the free radical scavenging behavior of a composite formed by tomato extract and LDH particles prepared by our method [19]. The main technique for the study was electron paramagnetic resonance spectroscopy, which provides information on unpaired electrons and easily identifies organic free radicals [23,24].

2. Materials and Methods

2.1. Tomato extract and layered double hydroxide (TE-LDH) preparation.

The composite material was prepared by alkaline precipitation of the LDH particles within the liquid tomato extract. Based on the dry composition and ideal formula $Mg_3Al(OH)NO_3$, the reagents were calculated to produce suspensions with 1.0, 1.25, 25, 50, and 75 mg of LDH per milliliter of tomato extract. Firstly, the peel and seed of red tomato (Solanum Lycopersicum) were removed with a knife; the resulting pulp was ground in a mortar, sieved through a 2 mm mesh, and 50.0 mL of this liquid was transferred to a vessel.

Separately, a solution was prepared by adding 2.336 g of $Mg(NO_3)_2 \cdot 6H_2O$ and 1.141 g of $Al(NO_3)_3 \cdot 6H_2O$ to 50 mL of water. The tomato juice and the salts solution were mixed under vigorous stirring and adjusted to pH = 8.4 with 1M NaOH solution. The suspension was stirred for 60 minutes. After that, the obtained solid was separated by centrifugation and washed with water until the liquid phase presented pH = 7.0. The solid was dried at 60 °C for 24 h. The product was labeled as TE-LDH. This experiment's magnesium and aluminum mass corresponds to 25 mg LDH / mL. The salt masses changed proportionally to prepare the samples with 1.0, 1.25, 50, and 75 mg of LDH/ mL.

The solid TE reference sample was prepared for the oxidation assays by drying the sieved pulp at 40 °C, while the $MgAl-NO_3$ LDH was prepared with magnesium and aluminum salts equivalent to the 25 mg LDH / mL sample and precipitated with NaOH solution in deionized water.

2.2. Characterization.

The X-ray diffraction analyses were conducted by placing the finely powdered samples in a glass sample holder. The patterns were collected in the 2Theta mode with a step of 0.02° at a scan rate of 40 s per step in a PANalytical diffractometer model EMPYREAN using Cu-Kα radiation. The infrared spectra were collected in the attenuated total reflectance mode with a Thermo Scientific spectrometer, model iS50 ATR. The spectra were averaged from 16 scans with 4 cm^{-1} of resolution. The morphology and composition were analyzed by scanning electron microscopy with a JEOL JSM 5400 LV microscope coupled to energy-dispersive X-ray spectroscopy (EDS) analyzer Bruker, model XFlash 6I30. The samples were irradiated with 20 kV. Considering that lycopene is the primary antioxidant component in tomatoes, it was quantified by high-performance liquid chromatography with Agilent Technologies equipment, model 1260 infinity. A Scientific ODS hypersil column (150 mm x 4.6 mm, 5 microns) was used at 25 °C. The ketone was used as a solvent, and each sample was analyzed in triplicate. The calibration curve was prepared with standards from 2 to 10 ppm giving a correlation factor of 0.9940. Free radicals formed in the composite were measured directly in the sample without the use of a scavenger [25]. The complete samples were transferred to a quartz tube and read at room temperature with a JEOL ESR spectrometer model FA200 operated in the X-band. The UV-Vis spectra were acquired with an Agilent Technologies apparatus with an integrating sphere, model Cary 300 UV-Vis.

2.3. Oxidation assays against H_2O_2.

The TE-LDH powder was separated into four plastic tubes and mixed with a 30% H_2O_2 solution in the amounts listed in Table 1 for 24 hours. The liquid was removed by decanting, and the solid was dried at 40 °C for 12 h.

Table 1. Relationship of TE-LDH composite mass and hydrogen peroxide.

Tube	TE-LDH (g)	30% H_2O_2 Solution (mL)
1	0.0121	0
2	0.0122	5
3	0.0121	10
4	0.0126	15

2.4. Antioxidant total capacity.

The antioxidant capacity was measured with the total antioxidant capacity (TAC) assay kit of Sigma-Aldrich. The assays were conducted in triplicate with 2.3 mg of sample to measure the activity to protect the oxidation of Cu^+ cations. The results were obtained from the color development at 450 nm and expressed as chemical equivalents of uric acid (eq UA). After 20 months of storage, the experiment was repeated for the TE-LDH composites.

3. Results and Discussion

3.1. Morphology and composition of TE-LDH composite.

The XRD analysis (figure 1a) indicate that samples prepared with 1.0 and 1.5 mg LDH/ mL of TE are amorphous materials owing to the wide signals between 18 and 40 (2 theta) degree [26]. These two samples were red films, and it was not possible to grind them with a mortar. The sample with 25 mg LDH/ mL presented incipient reflections of LDH particles (marked with an asterisk), which became more intense in the samples with 50 and 75 mg / mL. As previously reported, the reflections with an asterisk are clearly attributed to LDH structures[26,27]. Since the objective of this work was the assessment of the antioxidant behavior of the composite, and this is attributed to the tomato extract [28], the sample prepared with 25 mg / mL was selected as this contained the lowest identifiable content of LDH, and the powder was easily ground and handled in the fine powder form. The EDS mapping showed the distribution of magnesium, aluminum, and carbon content all along the micrograph, indicating that the LDH particles are uniformly distributed in the organic matter from the tomato (Figure 1a). As demonstrated in the SEM micrograph and histogram in Figure 1b, the composite presents a uniform size, an average 56 nm (SD. = 17, n = 40).
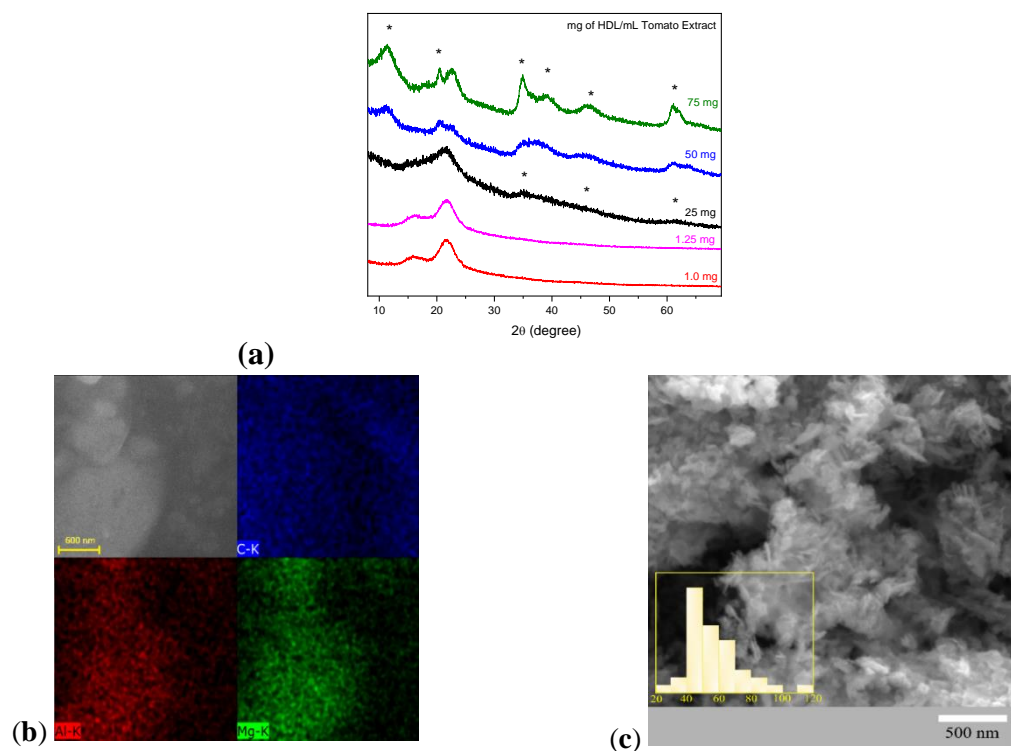

(a)

(b)

(c)

Figure 1. (**a**) X-ray diffraction patterns of the TE precipitated with different amounts of LDH; (**b**) EDS mapping; (**c**) the SEM micrograph of the TE-LDH composite precipitated with 25 mg LDH / mL of TE.

3.2. Total antioxidant activity of TE-LDH composite.

The total antioxidant activity of the composite was compared with the separate components and with a lycopene reference, as this is the main antioxidant agent in tomato fruit (Figure 2). While lycopene presented the highest activity of 2.3 EqUA, the capacity of TE was 0.77 EqUA indicating the presence of non-antioxidant components in the tomato pulp. The capacity in the composite decreases to 0.46 EqUA, which is proportional to the 18% lycopene content in the composite detected by HPLC. In other words, if the proportional amount of pure lycopene were compared with this 18% Lycopene, the expected value for the proportional content of lycopene would be 4.88 EqUA (dotted value in Figure 2). The isolated LDH sample presented a small activity of 0.10EqUA; practically, this did not contribute to the antioxidant activity of the TE-LDH composite. However, it does provide some stability to the composite since it can be observed that after 20 months of storage without special conditions, its antioxidant capacity decreases to 0.31 EqUA.
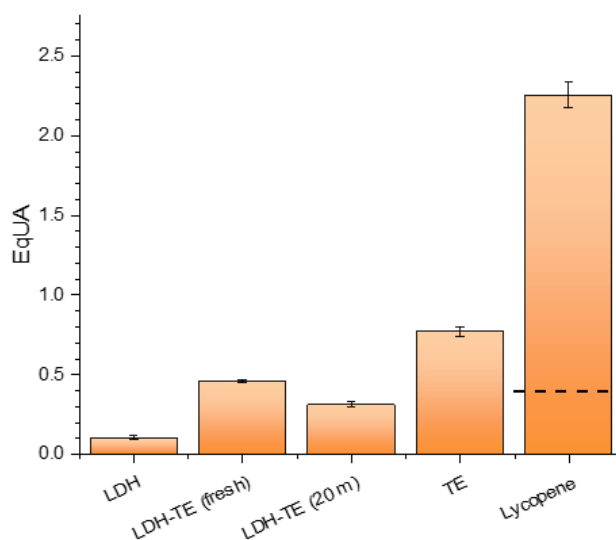

Figure 2. Total antioxidant capacity of the TE-LDH composite and the isolated components.

However, an EPR analysis was conducted on a pure LDH sample and its product from a reaction with 15 mL of H_2O_2 solution (Figure 3). The initial sample presented signals from an internal Mn^{2+} reference. After the reaction with H_2O_2, the spectrum showed a broad absorption signal with a g-factor close to 2.2, which is close to that found in the TE-LDH composite also reacted with 15 mL of H_2O_2 solution; therefore, the LDH particles spread along with the TE-LDH composite act as scavengers and stabilizers of free radicals and the influence is evidenced after the saturation of free radicals in the organic moiety. The presented results demonstrated that the TE-LDH composite could retain free radicals and stabilize them. However, there was no direct relationship with the antioxidant capacity, especially with pure lycopene.

The TE-LDH could be used as a scavenger system to sense the formation of radicals, for example, its addition to a polymer to prevent degradation through radical formation; in this way, the composite could protect against oxidation and simultaneously provide a probe to detect radicals. Another study needed for this composite is to determine the reactivity of the free radicals retained to act as neutralizers of radicals present in a polymer matrix or a tissue.
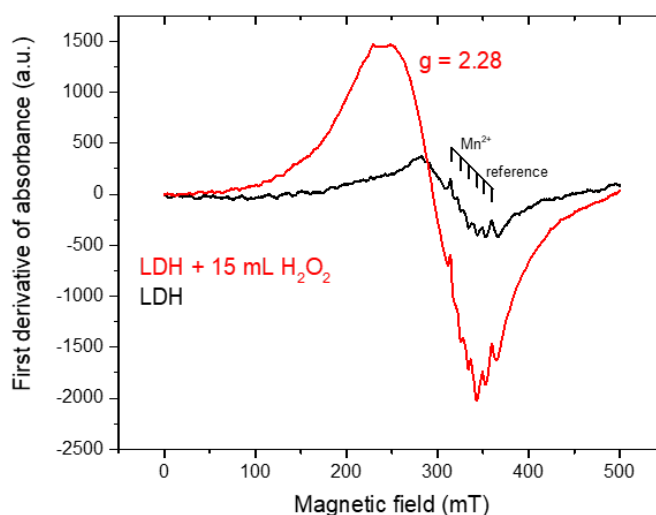
Figure 3. EPR spectrum of an isolated LDH sample before and after the reaction with the H_2O_2 solution.

3.3. EPR of TE-LDH composite treated with 30% H_2O_2 solution.

The EPR spectra of the samples treated with 30% H_2O_2 solution are presented in Figure 4. As it can be observed, the initial sample presented an absorption signal with g = 2.009, which is associated with organic free radicals [29–31], and the formation of free radicals in the composite where the unpaired electron is closer to carbon or oxygen atoms [32].
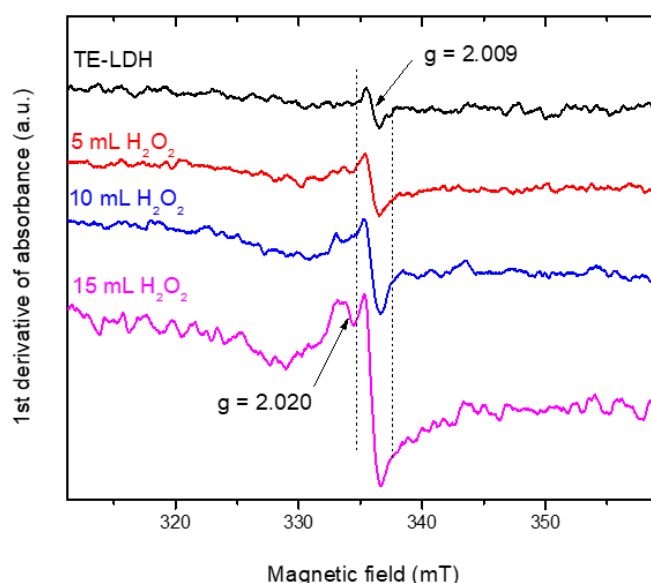

**Figure 4.** EPR spectra of TE-LDH composite treated with different volumes of 30% H_2O_2 solution.

A study conducted with gamma irradiation on tomatoes demonstrated that three absorption signals are observed when free radicals are distributed in the cellulose network [33]; such splitting is not found in our sample. Then, the free radical is probably located in a carbonaceous structure like lycopene. This supposition is probable, considering that the HPLC analysis revealed 18% of lycopene content.

The addition of H_2O_2 to the composite (Table 2) leads to i) an increase in the intensity and ii) a widening of the absorption signal, and these effects increase the area of the curve (Figure 5). The higher intensity results from a higher content of unpaired electrons, and it increased proportionally to the volume of H_2O_2 added to the composite. Then, the TE-LDH composite can retain the free radical produced by the peroxide.

Table 2. Width and area under the curve of the EPR absorption signal in the TE-LDH composite treated with different volumes of 30% H_2O_2 solution.

H_2O_2 (mL)	$B_{initial}$	B_{final}	ΔB (mT)	Area under the curve
TE-LDH	335.0	337.2	2.2	0.224
5	334.4	338.1	3.7	0.376
10	332.5	338.10	5.6	0.484
15	332.2	338.4	6.2	1.613

However, as the volume of H_2O_2 increased, the widening of the signal evidenced the appearance of a new g factor with a larger value; this effect indicates the unpaired electrons with a different local magnetic field [34]. The new g factor was identified in the sample treated with 15 mL H_2O_2 at g = 2.020.
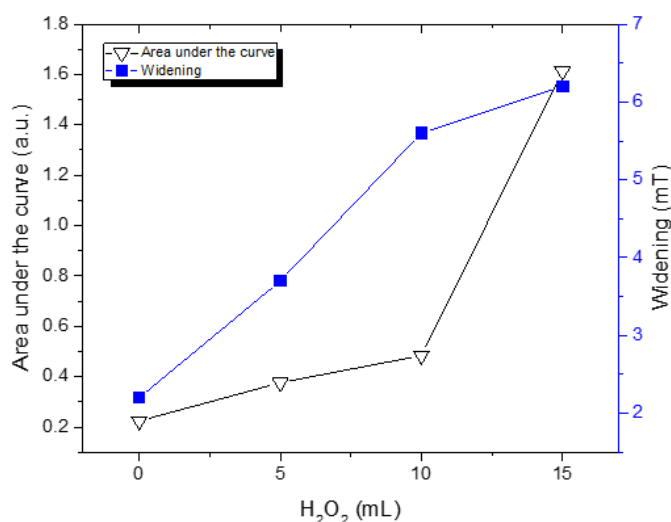
Figure 5. The increasing trend in the area under the curve and widening of the EPR signal influenced by the volume of the H_2O_2 solution. The volume at the zero point corresponds to the TE-LDH reference.

One report described the widening of more than 15 mT in the signal of organic free radicals from humic substances when paramagnetic ions (such as Fe^{3+}, Mn^{2+}, and Cu^{2+}) were present [35]; however, the addition of diamagnetic anions (such as Na^+, Zn^{2+}, and Al^{3+}) did not modify the signal at least in the concentration of 0.01%.

Larger contents of Zn^{2+} and Al^{3+}, as in the case of LDH structures, affect the absorption signal of interlayer nitrate ions by interaction with the aluminum nucleus (I = 5/2) [22], especially the observed g factor in LDH caused by nitrate ions reached values of 2.01 [36], in this literature report, another contribution arises from Zn(I) cations producing g = 2.1 [37].

3.4. Infrared and UV- Vis analysis of composites treated with H_2O_2 solution.

Once the EPR spectra indicated that the TE-LDH composite retained unpaired electrons, the samples were analyzed by infrared spectroscopy to identify the fragments that reacted with the peroxide radicals. In order to demonstrate the changes more clearly, the infrared spectra were divided into three regions and normalized, considering the band associated with the stretching of O-H bonds at 3300 cm^{-1} as reference (Figure 6). The first change of relative intensities is observed within the 4000-2500 cm^{-1} range; here, a set of bands from stretching of H-C-H bonds appear at 2920 cm^{-1}, the H-C=C vibration is included within this set [38], and the relative intensity decreases as the volume of H_2O_2 increases indicating that HO· radicals probable reacted with unsaturations in the TE. A second region between 1800 and 1300 cm^{-1} contains an intense band at 1630 cm^{-1}, which has been associated with the

stretching of H-C=C bonds in lycopene [38], similarly to a region in the 1000-900 cm^{-1} range containing a weak signal at 950 cm^{-1}, which has also been associated to the stretching of C=C in carotenoids of tomato fruits [39].

The intensity of both signals decreases when the volume of H_2O_2 increases, in agreement with the reaction of the unsaturations with the attack of HO$^{\cdot}$ radicals, either forming new bonds or merely breaking the unsaturation and forming an organic radical as represented in Figure 7.

The UV-vis spectra collected directly from the solid also support the proposed reaction. The spectrum of the TE-LDH presents a set of three bands between 430 and 483 nm (identified with three red dotted lines in Figure 6d that match the spectra of carotenoids from tomato and orange [38,40,41]; the absorption of these signals felt with the addition of H_2O_2 solution.
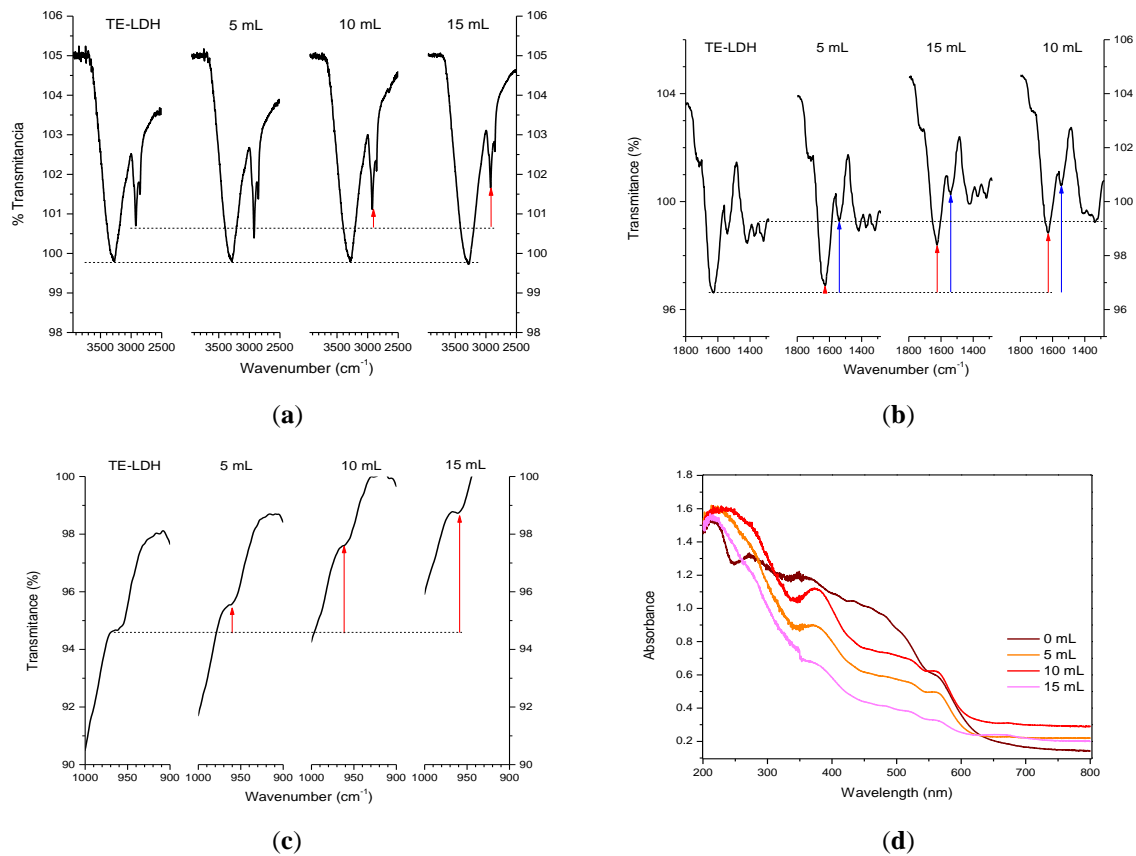

(a)

(b)

(c)

(d)

Figure 6. IR spectra of TE-LDH composites treated with different volumes of 30% H_2O_2 solution (**a**) zone 3500 -2500 cm^{-1}; (**b**) zone 1800 -1300 cm^{-1}; (**c**) zone 1000-900 cm^{-1}; (**d**) UV-vis spectra of the TE-LDH composite attacked with different volumes of 30% H_2O_2 solution.
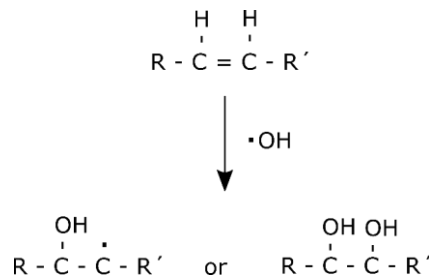

Figure 7. The proposed reaction between the unsaturated regions in the TE-LDH composite and the radicals provided by the H_2O_2 solution.

3.5. X-ray diffraction of composites treated with H_2O_2 solution.

The X-ray diffraction profile of the TE-LDH composite described in Figure 1a is compared with the profiles of the samples exposed to the H_2O_2 solution (Figure 8). The low-intensity signals are observed due to the low content and small size of the LDH particles, but mainly, the preferential intensity of reflection at 35 and 62 degrees (marked with asterisks) are typically observed in delaminated LDH [42]. Therefore, this XRD profile indicates that the TE allows LDH sheets to form but limits their stacking at 25 mg/mL concentration.

The samples treated with the lowest and highest volume of H_2O_2 solution were analyzed, and no changes were detected, suggesting that the crystalline part of the composite was not affected. The changes in the reaction occurred at the molecular level.
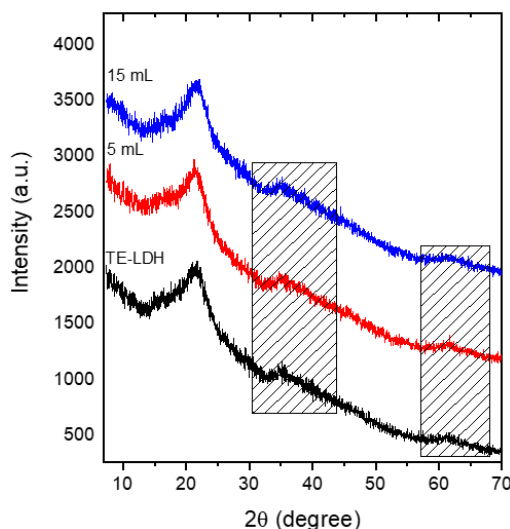

Figure 8. X-ray diffraction profiles of the TE-LDH composite before and after the reaction with different volumes of 30% H_2O_2 solution.

4. Conclusions

The composite is formed by a uniform distribution of MgAl-NO$_3$ LDH nanoparticles along with the TE matrix, where there is a lycopene content of 18%. Lycopene is the first responsible for free radical scavenging when exposed to the lowest concentration of H_2O_2, as demonstrated by infrared and EPR spectroscopy. The OH· radicals reacted with unsaturations in the TE-LDH composite and formed stable organic radicals for days. When the concentration of H_2O_2 increases, the free radicals are also transferred and concentrated in the LDH particles. The intimate and uniform distribution of LDH particles in the organic components of the TE leads to an interaction that enables a transfer of unpaired electrons between TE and MgAl-NO$_3$ LDH. The unpaired electron in the MgAl-NO$_3$ LDH is likely reducing aluminum sites.

The scavenging ability of the TE-LDH composite could help to use it as a probe to identify free radicals if it were added to a liquid system or a solid material, especially in polymers where the TE-LDH could be easily incorporated.

Funding

Acknowledgments

Conflicts of Interest

The authors declare no conflict of interest.

References

1. Quintanar Escorza, M.A.; Calderón Salinas, J.V. La Capacidad Antioxidante Total. Bases y Aplicaciones. *Revista de Educación Bioquímica* **2009**, *28*, 89–101.

2. Przybylska, S.; Tokarczyk, G. Lycopene in the Prevention of Cardiovascular Diseases. *International Journal of Molecular Sciences* **2022**, *23*, 1957, https://doi.org/10.3390/ijms23041957.

3. Bin-Jumah, M.N.; Nadeem, M.S.; Gilani, S.J.; Mubeen, B.; Ullah, I.; Alzarea, S.I.; Ghoneim, M.M.; Alshehri, S.; Al-Abbasi, F.A.; Kazmi, I. Lycopene: A Natural Arsenal in the War against Oxidative Stress and Cardiovascular Diseases. *Antioxidants* **2022**, *11*, 232, https://doi.org/10.3390/antiox11020232.

4. Sarker, U.; Hossain, Md. M.; Oba, S. Nutritional and Antioxidant Components and Antioxidant Capacity in Green Morph Amaranthus Leafy Vegetable. *Scientific Reports* **2020**, *10*, 1336, https://doi.org/10.1038/s41598-020-57687-3.

5. Eh, A.L.S.; Teoh, S.G. Novel Modified Ultrasonication Technique for the Extraction of Lycopene from Tomatoes. *Ultrasonics Sonochemistry* **2012**, *19*, 151–159, https://doi.org/10.1016/j.ultsonch.2011.05.019.

6. Poojary, M.M.; Passamonti, P. Extraction of Lycopene from Tomato Processing Waste: Kinetics and Modelling. *Food Chemistry* **2015**, *173*, 943–950, https://doi.org/10.1016/j.foodchem.2014.10.127.

7. Amorim, A.d.G.N.; Vasconcelos, A. G.; Souza, J.; Oliveira, A.; Gullón, B.; de Souza de Almeida Leite, J. R.; Pintado, M. Bio-Availability, Anticancer Potential, and Chemical Data of Lycopene: An Overview and Technological Prospecting. *Antioxidants* **2022**, *11*, 360, https://doi.org/10.3390/antiox11020360.

8. Laranjeira, T.; Costa, A.; Faria-Silva, C.; Ribeiro, D.; de Oliveira, J.M.P.F.; Simões, S.; Ascenso, A. Sustainable Valorization of Tomato By-Products to Obtain Bioactive Compounds: Their Potential in Inflammation and Cancer Management. *Molecules* **2022**, *27*, 1701, https://doi.org/10.3390/molecules27051701.

9. Gomez, N.A.G.; Wypych, F. Nanocomposites of Polyethylene and Ternary (Mg + Zn/Al) Layered Double Hydroxide Modified with an Organic UV Absorber. *Journal of Polymer Research* **2019**, *26*, 203, https://doi.org/10.1007/s10965-019-1868-4.

10. Assis, R.Q.; Rios, P.D.; Rios, A.d.O.; Olivera, F.C. Biodegradable Packaging of Cellulose Acetate Incorporated with Norbixin, Lycopene or Zeaxanthin. *Industrial Crops and Products* **2020**, *147*, 112212, https://doi.org/10.1016/j.indcrop.2020.112212.

11. Assis, R.Q.; Lopes, S.M.; Costa, T.M.H.; Flôres, S.H.; Rios, A. de O. Active Biodegradable Cassava Starch Films Incorporated Lycopene Nanocapsules. *Industrial Crops and Products* **2017**, *109*, 818–827, https://doi.org/10.1016/j.indcrop.2017.09.043.

12. Pereira, R.C.; Carneiro, J. de D.S.; Assis, O.B.; Borges, S.V. Mechanical and Structural Characterization of Whey Protein Concentrate/Montmorillonite/Lycopene Films. *Journal of the Science of Food and Agriculture* **2017**, *97*, 4978–4986, https://doi.org/10.1002/jsfa.8376.

13. Asadi, S.; Pirsa, S. Production of Biodegradable Film Based on Polylactic Acid, Modified with Lycopene Pigment and TiO2 and Studying Its Physicochemical Properties. *Journal of Polymers and the Environment* **2020**, *28*, 433–444, https://doi.org/10.1007/s10924-019-01618-5.

14. Chaudhary, B.U.; Lingayat, S.; Banerjee, A.N.; Kale, R.D. Development of Multifunctional Food Packaging Films Based on Waste Garlic Peel Extract and Chitosan. *International Journal of Biological Macromolecules* **2021**, *192*, 479–490, https://doi.org/10.1016/j.ijbiomac.2021.10.031.

15. Sadeghi, A.; Razavi, S.M.A.; Shahrampour, D. Fabrication and Characterization of Biodegradable Active Films with Modified Morphology Based on Polycaprolactone-Polylactic Acid-Green Tea Extract. *International Journal of Biological Macromolecules* **2022**, *205*, 341–356, https://doi.org/10.1016/j.ijbiomac.2022.02.070.

16. Bayer, G.; Shayganpour, A.; Zia, J.; Bayer, I.S. Polyvinyl Alcohol-Based Films Plasticized with an Edible Sweetened Gel Enriched with Antioxidant Carminic Acid. *Journal of Food Engineering* **2022**, *323*, 111000, https://doi.org/10.1016/j.jfoodeng.2022.111000.

17. Joshi, B.; Kar, S. K.; Yadav, P. K.; Yadav, S.; Shrestha, L.; Bera, T. K. Therapeutic and Medicinal Uses of Lycopene: A Systematic Review. *International Journal of Research in Medical Sciences* **2020**, *8*, 1195, https://doi.org/10.18203/2320-6012.ijrms20200804.

18. Wen, W.; Chen, X.; Huang, Z.; Chen, D.; Yu, B.; He, J.; Luo, Y.; Yan, H.; Chen, H.; Zheng, P.; Yu, J. Dietary Lycopene Supplementation Improves Meat Quality, Antioxidant Capacity and Skeletal Muscle Fiber Type Transformation in Finishing Pigs. *Animal Nutrition* **2022**, *8*, 256–264, https://doi.org/10.1016/j.aninu.2021.06.012.

19. Hernández, D.E.; Magallon, A.P.; Carbajal Arízaga, G.G. Green Extraction of Lycopene from Tomato Juice with Layered Double Hydroxide Nanoparticles. *Micro & Nano Letters* **2019**, *14*, 230–233, https://doi.org/10.1049/mnl.2018.5437.

20. He, L.; Zhi, J.; Li, H.; Jia, Y.; Gao, Q.; Wang, J.; Xu, Y.; Li, X. Peroxymonosulfate Activation by Magnetic NiCo Layered Double Hydroxides for Naproxen Degradation. *Colloids and Surfaces A: Physicochemical and Engineering Aspects* **2022**, *642*, 128696, https://doi.org/10.1016/j.colsurfa.2022.128696.

21. Wang, X.; Cheng, B.; Zhang, L.; Yu, J.; Li, Y. Synthesis of MgNiCo LDH Hollow Structure Derived from ZIF-67 as Superb Adsorbent for Congo Red. *Journal of Colloid and Interface Science* **2022**, *612*, 598–607. https://doi.org/10.1016/j.jcis.2021.12.176.

22. Izbudak, B.; Cecen, B.; Anaya, I.; Miri, A.K.; Bal-Ozturk, A.; Karaoz, E. Layered Double Hydroxide-Based Nanocomposite Scaffolds in Tissue Engineering Applications. *RSC Advances* **2021**, *11*, 30237–30252, https://doi.org/10.1039/D1RA03978D.

23. Nikolic, I.; Mitsou, E.; Damjanovic, A.; Papadimitriou, V.; Antic-Stankovic, J.; Stanojevic, B.; Xenakis, A.; Savic, S. Curcumin-Loaded Low-Energy Nanoemulsions: Linking EPR Spectroscopy-Analysed Microstructure and Antioxidant Potential with in Vitro Evaluated Biological Activity. *Journal of Molecular Liquids* **2020**, *301*, 112479, https://doi.org/10.1016/j.molliq.2020.112479.

24. Drouza, C.; Spanou, S.; Keramidas, A. EPR Methods Applied on Food Analysis. In *Topics From EPR Research*; IntechOpen, **2019**, https://doi.org/10.5772/intechopen.79844.

25. Pirker, K.F.; Reichenauer, T.G.; Pascual, E.C.; Kiefer, S.; Soja, G.; Goodman, B.A. Steady State Levels of Free Radicals in Tomato Fruit Exposed to Drought and Ozone Stress in a Field Experiment. *Plant Physiology and Biochemistry* **2003**, *41*, 921–927, https://doi.org/10.1016/S0981-9428(03)00137-2.

26. Ghanbari, N.; Ghafuri, H. Design and Preparation the Novel Polymeric Layered Double Hydroxide Nanocomposite (LDH/Polymer) as an Efficient and Recyclable Adsorbent for the Removal of Methylene Blue Dye from Water. *Environmental Technology & Innovation* **2022**, *26*, 102377, https://doi.org/10.1016/j.eti.2022.102377.

27. Shabani, S.; Dinari, M. Itaconic Acid-Modified Layered Double Hydroxide/Gellan Gum Nanocomposites for Congo Red Adsorption. *Scientific Reports* **2022**, *12*, 4356, https://doi.org/10.1038/s41598-022-08414-7.

28. Chada, P.S.N.; Santos, P.H.; Rodrigues, L.G.G.; Goulart, G.A.S.; Azevedo dos Santos, J.D.; Maraschin, M.; Lanza, M. Non-Conventional Techniques for the Extraction of Antioxidant Compounds and Lycopene from Industrial Tomato Pomace (Solanum Lycopersicum L.) Using Spouted Bed Drying as a Pre-Treatment. *Food Chemistry: X* **2022**, *13*, 100237, https://doi.org/10.1016/j.fochx.2022.100237.

29. Komosinska-Vassev, K.; Olczyk, P.; Kasperczyk, J.; Pilawa, B.; Krzyminiewski, R.; Dobosz, B.; Ramos, P.; Stojko, J.; Stojko, M.; Ivanova, D.; Olczyk, K. EPR Spectroscopic Examination of Different Types of Paramagnetic Centers in the Blood in the Course of Burn Healing. *Oxidative Medicine and Cellular Longevity* **2019**, *2019*, 7506274, https://doi.org/10.1155/2019/7506274.

30. Pierzchała, E.; Ramos, P.; Pilawa, B. Application of EPR Spectroscopy in Comparative Analysis of Free Radicals Thermally Formed during Storage in the Antibacterial Ointments Containing Fusidic Acid and Neomycin. *Acta Poloniae Pharmaceutica - Drug Research* **2017**, *74*, 1071–1078.

31. Shi, D.; Xia, C.; Liu, C. Photoinduced Transition-Metal-Free Alkynylation of Alkyl Pinacol Boronates. *CCS Chemistry* **2021**, *3*, 1718–1728, https://doi.org/10.31635/ccschem.020.202000371.

32. Pierzchala, E.; Ramos, P.; Pilawa, B. EPR Study of Free Radicals Formed in Fusidic Acid and Neomycin under UV Irradiation. *Acta Poloniae Pharmaceutica - Drug Research* **2019**, *76*, 215–223, https://doi.org/10.32383/appdr/96299.

33. Aleksieva, K.; Georgieva, L.; Tzvetkova, E.; Yordanov, N.D. EPR Study on Tomatoes before and after Gamma-Irradiation. *Radiation Physics and Chemistry* **2009**, *78*, 823–825, https://doi.org/10.1016/j.radphyschem.2009.05.013.

34. Yi, P.; Chen, Q.; Li, H.; Lang, D.; Zhao, Q.; Pan, B.; Xing, B. A Comparative Study on the Formation of Environmentally Persistent Free Radicals (EPFRs) on Hematite and Goethite: Contribution of Various Catechol Degradation Byproducts. *Environmental Science and Technology* **2019**, *53*, 13713–13719, https://doi.org/10.1021/acs.est.9b04444.

35. Novotny, E.H.; Martin-Neto, L. Effects of Humidity and Metal Ions on the Free Radicals Analysis of Peat Humus. *Geoderma* **2002**, *106*, 305–317, https://doi.org/10.1016/S0016-7061(01)00130-6.

36. Ali Ahmed, A.A.; Abidin Talib, Z.; Hussein, M.Z.b. ESR Spectra and Thermal Diffusivity of ZnAl Layered Double Hydroxide. *Journal of Physics and Chemistry of Solids* **2012**, *73*, 124–128, https://doi.org/10.1016/j.jpcs.2011.10.016.

37. Yu, B.; Zhu, C.; Gan, F.; Huang, Y. Electron Spin Resonance Properties of ZnO Microcrystallites. *Materials Letters* **1998**, *33*, 247–250, https://doi.org/10.1016/S0167-577X(97)00117-1.

38. Aghel, N.; Ramezani, Z.; Amirfakhrian, S. Isolation and Quantification of Lycopene from Tomato Cultivated in Dezfoul, Iran. *Jundishapur Journal of Natural Pharmaceutical Products* **2011**, *6*, 9–15.

39. Baranska, M.; Schütze, W.; Schulz, H. Determination of Lycopene and β-Carotene Content in Tomato Fruits and Related Products: Comparison of FT-Raman, ATR-IR, and NIR Spectroscopy. *Analytical Chemistry* **2006**, *78*, 8456–8461, https://doi.org/10.1021/ac061220j.

40. Chemat-Djenni, Z.; Ferhat, M. A.; Tomao, V.; Chemat, F. Carotenoid Extraction from Tomato Using a Green Solvent Resulting from Orange Processing Waste. *Journal of Essential Oil Bearing Plants* **2010**, *13*, 139–147, https://doi.org/10.1080/0972060X.2010.10643803.

41. Popescu, M.; Iancu, P.; Pleșu, V.; Bîldea, C.S.; Todasca, C.M. Different Spectrophotometric Methods for Simultaneous Quantification of Lycopene and β-Carotene from a Binary Mixture. *LWT* **2022**, *160*, 113238, https://doi.org/10.1016/j.lwt.2022.113238.

42. Zhang, Y.; Xu, H.; Lu, S. Preparation and Application of Layered Double Hydroxide Nanosheets. *RSC Advances* **2021**, *11*, 24254–24281, https://doi.org/10.1039/D1RA03289E.
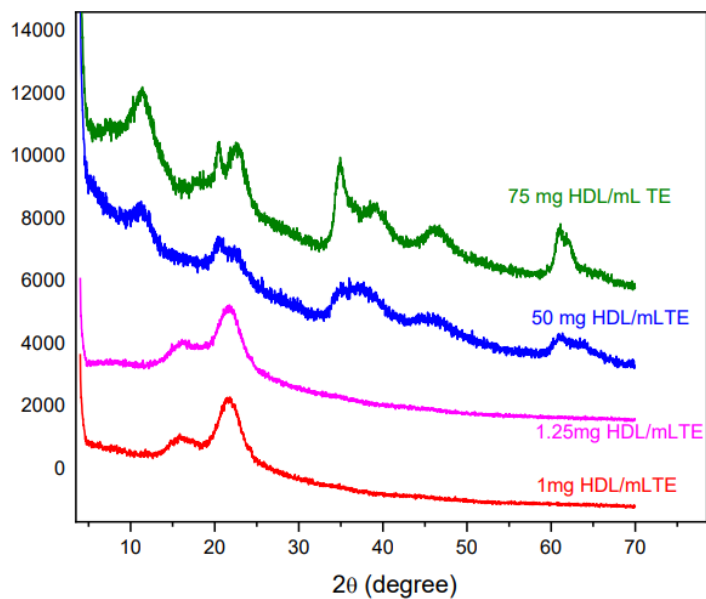
Supplementary information

Figure S1. XRD patterns of composites prepared with a different mass of LDH per one milliliter of tomato extract (TE). The profiles of samples with 1 and 1.25 mg/mL produce the quase-amorphous pattern with width signals. On the contrary, the increase to 50 and 75 mg/mL gives clearer evidence if the LDH presence with the typical reflections matching with an LDH structure, such as recorded in the 9012627 cif file.